Supplementary Information

Dysregulation of Autophagy in Chronic Lymphocytic Leukemia with the Small-molecule Sirtuin inhibitor Tenovin-6

Stephanie F MacCallum, Michael J Groves, John James, Karen Murray, Virginia Appleyard, Alan R Prescott, Abed A Drbal, Anna Nicolaou, Joan Cunningham, Sally Haydock, Ian G Ganley, Nicholas J Westwood, Philip J Coates, Sonia Lain, Sudhir Tauro

Supplementary Figure 1. SirT1 expression in CLL cells. Patterns of SirT1 expression in 5 representative CLL specimens (1-5) are shown in the gel image. Human blood lymphocytes did not express significant levels of SirT1 and constituted the negative control (-). Whole cell lysates of the human breast cancer cell line MCF7 provided protein for the positive control (+).

Supplementary Figure 2. Intracellular protein expression in Tnv-6-treated CLL cells. The Western blot gel images show expression of p53, acetylated histone H4 (acet-H4), acetylated p53 (acet-p53), acetylated tubulin (acet-tubulin) and phosphorylated H2AX (phospho-H2AX) in Tnv-6-treated cells (Tnv-6) compared to untreated (Cntrl) cultures. The heterogeneity in p53 (a) and acet-H4 (b) expression-levels is exemplified in cultures from 3 and 2 patient respectively, but p53 induction was consistently observed in fludarabine-treated cultures (fludara) (a). Expression of acet-p53 (c), acet-tubulin (d) and phosphor-H2AX (e) remained unchanged in all patients. To ensure validity of the Western blot assay, positive controls (+) were used for each protein: for acetylated-H4, extracts from HT29 colorectal cell-line lysates irradiated with 5Gy; for acetylated-p53, HeLa cell extracts cultured with 400nM TSA and Doxyrubicin (0.5μM) for 24 hours; for acetylated-tubulin, protein from the JURKAT leukemic cell-line treated with TSA (40nM) for 16 hours and for phosphorylated-H2AX, CLL cells cultured with fludarabine for 24 hours.

Supplementary Figure 3. Global gene expression profiling of CLL cells treated with Tnv-6, TSA and combination Tnv-6 and TSA. Analysis of the transcriptome of CLL cells from 5 patients identifies a pattern of gene expression following Tnv-6 (Tnv) treatment that is distinct from the profile of untreated (Con) cells and cells cultured with TSA or combined therapy with Tnv-6 plus TSA (T+T). Based on the expression profiles, two distinct clusters are identified (a): in the first, there is a clear distinction between the expression profiles of Con and Tnv-6-treated cells. Within the second cluster, each of the five patients forms a unique sub-branch, in which combined treatment consistently leads to an overall gene expression profile that is closer to the Tnv-6 cluster. Numbers (1-5) can be used to identify individual patients and follow changes in gene expression in response to different drugs. The ability of TSA to affect the expression of a larger number of genes (red circle) compared to Tnv-6 (yellow circle) is demonstrated by the Venn diagram in (b). Both agents had the capacity to influence changes in 107 genes, but combination therapy altered the expression of a unique set of 468 genes, not regulated by Tnv- or TSA as single agents.

Supplementary Figure 4. Real-time PCR validation of increased cholesterol bio-synthetic transcriptional activity following Tnv-6 treatment. The activity of 3-hydroxy-3-methyl-glutaryl-CoA reductase (*HMGCR*) and Lanosterol synthase (*LSS*) and their transcriptional regulators Sterol Regulatory Element-Binding Proteins **(***SREBPs***)** identified in global gene expression profiles of Tnv-6 treated cells was measured by RT-PCR and (n=6) and normalized to GAPDH. Results (mean fold increases ± sd) are expressed relative to corresponding controls (assigned a value of 1). Increased transcription of *HMGCR* (p=0.01), *LSS* (p=0.007), *SREBP-1* (p=0.06) and *SREBP-2* (p=0.001, Student's t-test) was observed in cells exposed to Tnv-6.

Supplementary Figure 5. Changes in LC3 flux with Tnv-6 compared with known stimulators and inhibitors of autophagy. This representative example (of three specimens tested) shows a comparable increase in LC3-II expression with Tnv-6, bafilomycin-A (Baf-A) or combination treatment with Tnv-6 and bafilomycin-A compared to untreated (control) cells. By contrast, the pattern of LC3 flux with Ku-0063794 (Ku) was different and a trend towards synergistic increase in LC3-II was evident when Tnv-6 was combined with Ku-0063794 (p=0.06, by analysis of protein band-density relative to actin n=3).

Supplementary Figure 6: Changes in LC3 expression in cells with del(17p) CLL studied by fluorescence microscopy. LC3 expression-intensity following Tnv-6 treatment was investigated by staining cytospin preparations of cells fixed with 4% formaldehyde and permeabilized with 0.2% Triton X-100, sequentially with mouse anti-LC3 primary antibody (MBL, Massachusetts, USA), Alexa-Fluor-labelled goat anti-mouse secondary antibody (Life Technologies, Paisely, UK) and DAPI/Antifade (Vysis). Stained cells were evaluated using an Olympus BX60 (Olympus UK Ltd, Southend-on-Sea, UK) epifluorescence microscope equipped with the appropriate filter sets and changes in fluorescence were compared with untreated (control) cells at 60x magnification. Compared to control cultures (a), the LC3 fluoresce intensity (quantified using Image J software) indicating dysregulated autophagy was 2-fold greater in Tnv-6-treated cells (b).

Supplementary Table 1: Differential expression of genes following treatment of CLL cells with Tnv-6, TSA or Tnv-6 in combination with TSA, compared to control cultures. A total of 450 probe sets were identified as differentially expressed between Tnv-6-treated and control cultures [Supplemental Table 1(a)]. In comparison, twice as many gene probe sets (944) were identified in TSA-treated cells compared to control cells [Supplemental Table (1b)]. In combination, Tnv-6 and TSA affected the expression levels of 1364 gene probe sets compared to control cells [Supplemental Table 1(c)].

Supplementary Figure-1 (Tauro)

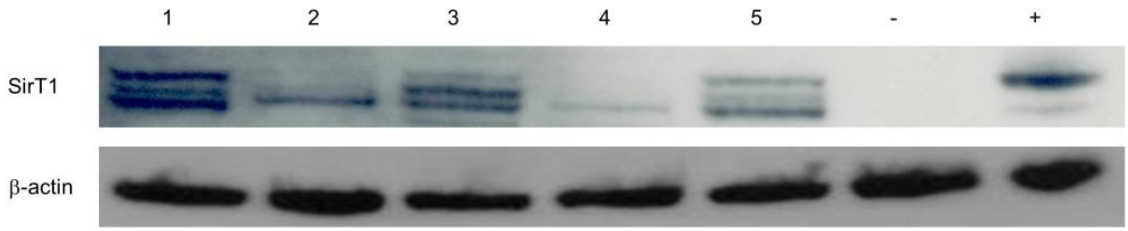

Supplementary Figure-2 (Tauro)

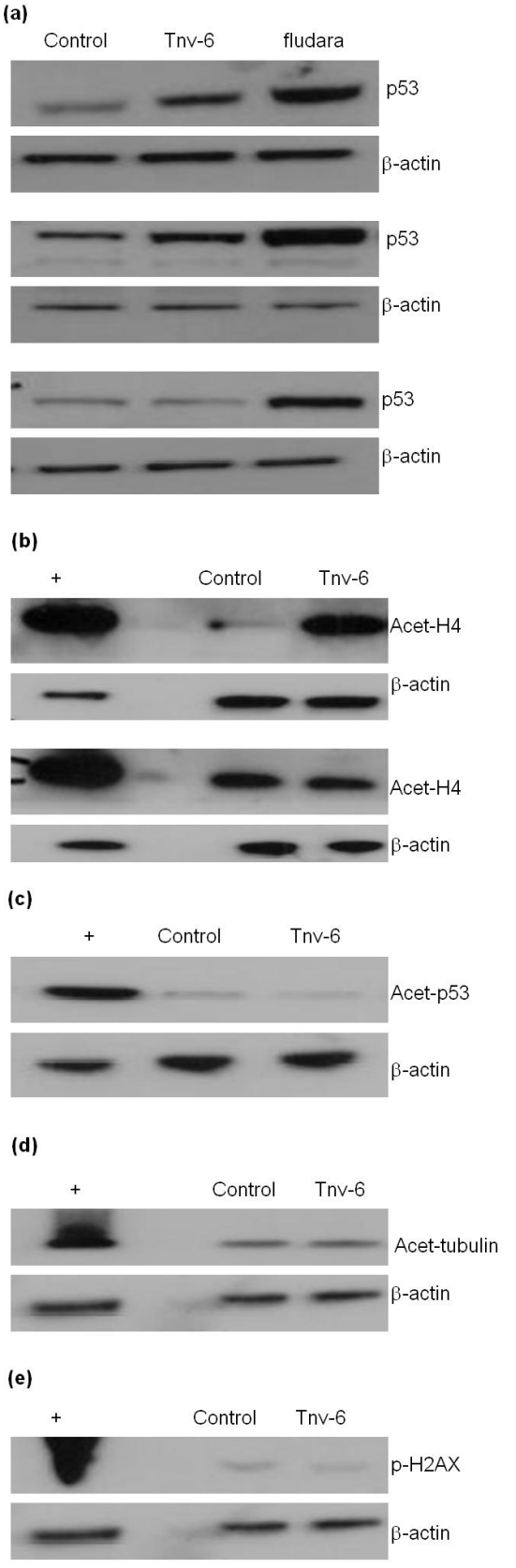

Supplementary Figure-3 (Tauro)

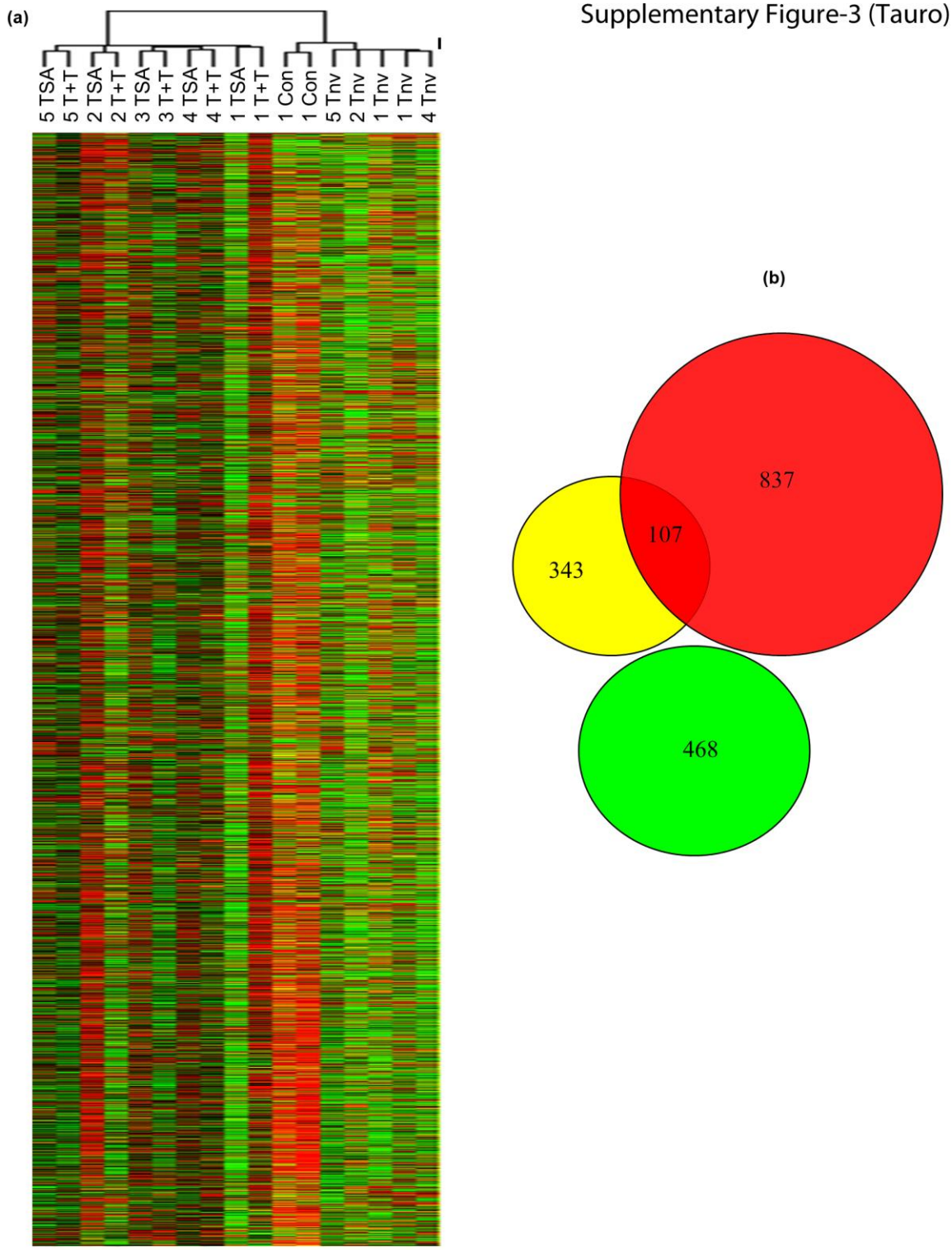

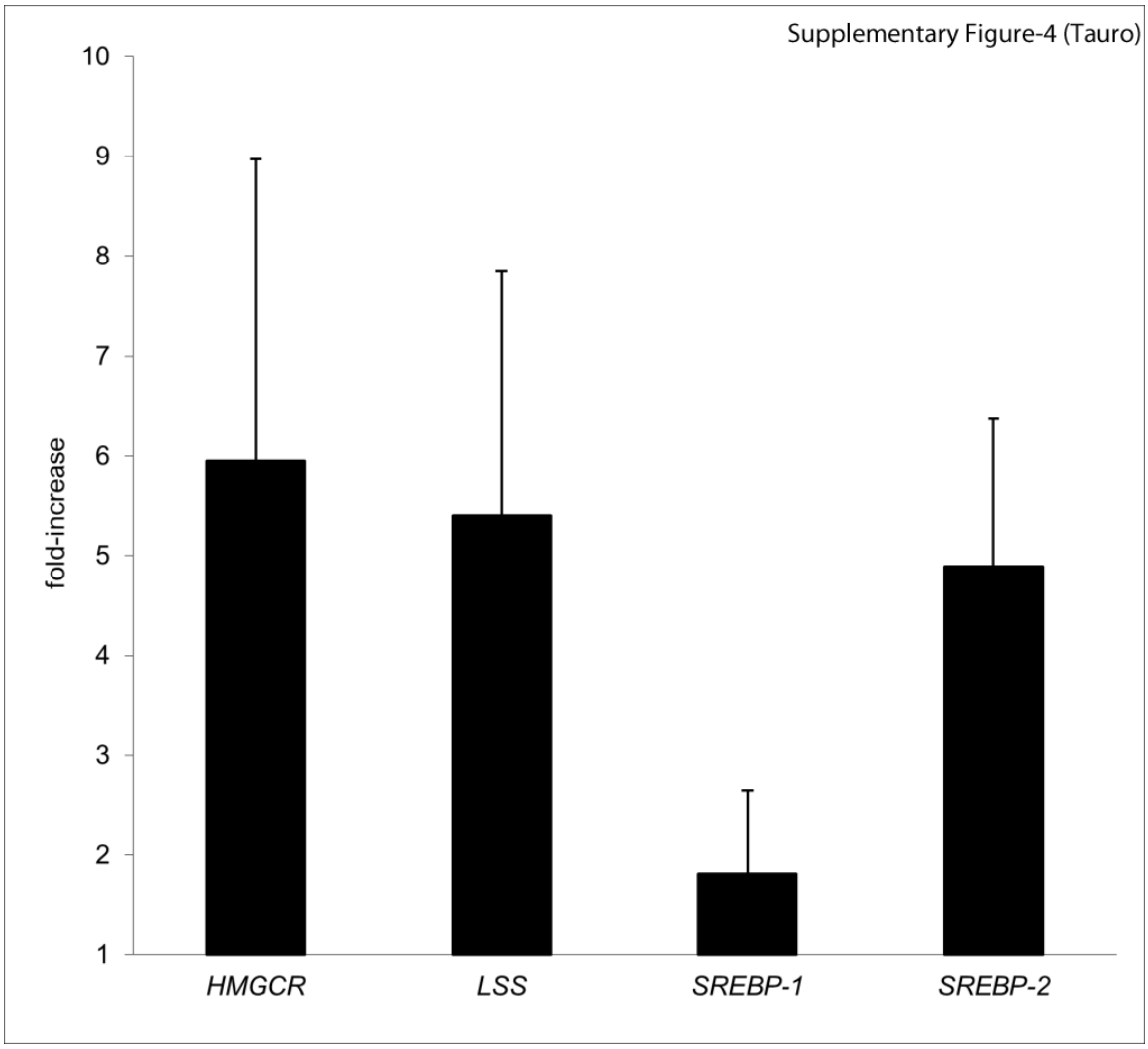
Supplementary Figure-4 (Tauro)
fold-increase
10
9
8
7
6
5
4
3
2
1
HMGCR
LSS
SREBP-1
SREBP-2

Supplementary Figure-5 (Tauro)

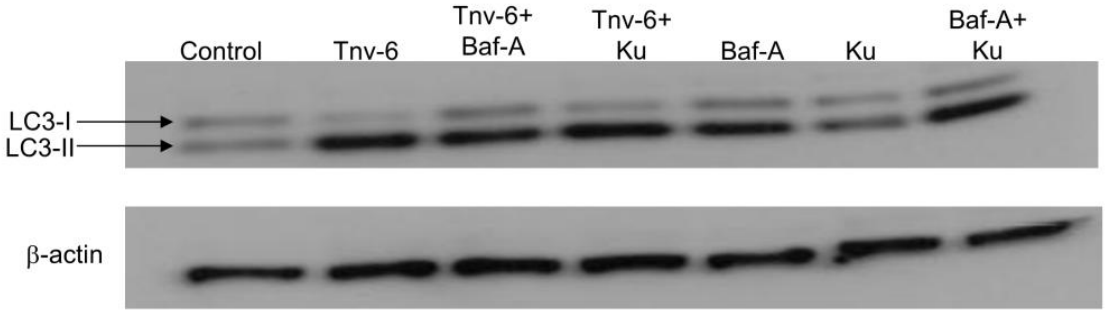

Supplementary Figure-6 (Tauro)